Optica Applicata, Vol. XIX, No. 3, 1989

Concentration characteristics of a seasonally adjusted circular cylindrical solar concentrator

PUNITA TANEJA, S. S. MATHUR, T. C. KANDPAL

Centre for Energy Studies, Indian Institute of Technology, Hauz Khas, New Delhi–110016, India.

Concentration characteristics of a circular cylindrical solar concentrators have been studied for two absorber configurations: flat-horizontal and flat-vertical. Conventional ray tracing technique has been used for this purpose. Since the concentrator is operated in a seasonally adjusted mode the LCR distribution curves have been plotted for different values of incidence angles. The effect of the mirror rim angle, absorber defocusing, lateral shift and the shading caused by the absorber, on the concentration characteritics have also been investigated.

1. Introduction

Solar concentrators are used in solar thermal applications for producing intermediate and high temperatures. Solar concentrators are either of fully tracking- or seasonally tracking-type. The latter provide operating temperatures in the range of 80°–200° C. The first effort towards the development of such a concentrator was probably made by TABOR and ZEIMER [1] who have shown that, for the average up to large acceptance angles, a circular profile produces a better overall focusing than a parabolic one. Moreover, a circular profile is designed easier, has a higher rigidity and is less expensive. The concentration characteristics of a seasonally tracked circular cylindrical solar concentrator (aligned in the East-West direction), obtained by using conventional ray tracing technique, are presented in this paper. Its purpose was a study of the optical performance of such concentrators for efficient collection of solar energy. Therefore, in this analysis, the optical aberrations of the mirror which play a significant role in conventional optical instruments have not been taken into account, since their impact on the solar energy collection characteristics of seasonally tracked solar concentrators in negligible. Two different absorber configurations are considered: flat-horizontal and flat-vertical. The flat-horizontal absorber is placed in the paraxial focal plane of the mirror, whereas the flat-vertical absorber is aligned along its optical axis. The effect of various design and operational parameters, including mirror rim angle, angle of incidence of solar radiation and the defocusing (lateral shift of the absorber) on the concentration characteristics is also investigated.

2. Ray trace analysis

The ray trace analysis is performed under the following assumptions:

1. The sun is a point source.
2. The mirror surface is specularly reflecting with a reflectance of 0.9.

3. The concentrator has a cylindrical symmetry. Hence the results obtained for one cross-section (in the x-y plane) may be extended to the complete length of the concentrator.

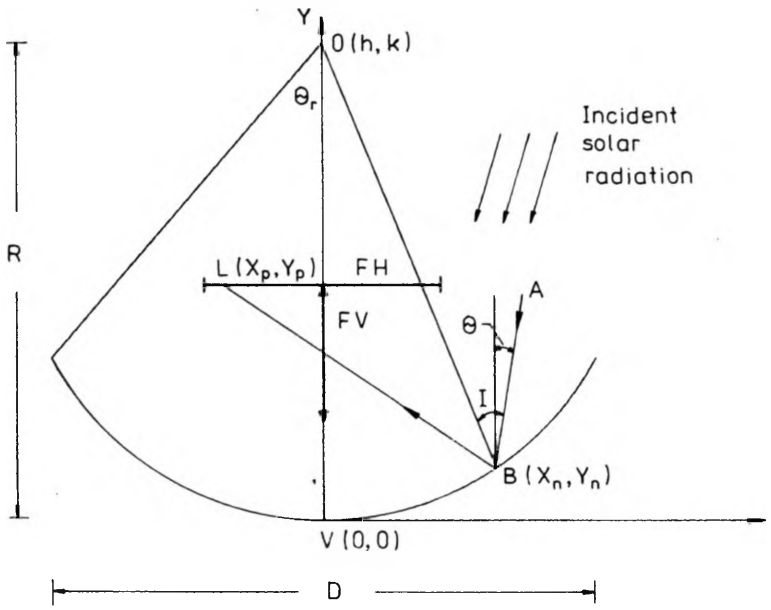

Fig. 1. Cross-section of a circular cylindrical solar concentrator showning both flat-horizontal (FH) and flat-vertical (FV) absorbers

Figure 1 illustrates a cross-section of circular cylindrical solar concentrator. In this diagram, both the flat-horizontal and flat-vertical absorbers are shown as straight line segments. The relation between the relative aperture (D/f) and the mirror rim angle θ_r is the following:

$$D/f = 2\sin\theta_r \tag{1}$$

where D denotes the mirror (aperture) diameter of curvature radius R and of the paraxial focal length f.

In this ray trace technique, the path of the ray runs from the point of its incidence on the mirror surface to the point where it is finally intercepted by the absorber's surface. The mirror aperture D is divided into a large number N of equal sections and one ray is made incident on each section (Fig. 1). The coordinates of the point B, where the ray AB is incident on the n-th section of the aperture, can be expressed by the following equation:

$$X_n = nD/N, \tag{2}$$

$$Y_n = [R^2 - X_n^2]^{1/2} \tag{3}$$

The angle of incidence I made by the ray (AB) with the normal $(B0)$ at the point B (X_n, Y_n) is

$$I = \tan^{-1}\left[\frac{\cot\theta - \{(Y_n - k)/(X_n - h)\}}{1 + \cot\theta\{(Y_n - k)/(X_n - h)\}}\right] \tag{4}$$

where h, k represent the coordinates of the centre of curvature of the mirror and θ represents the angle made by the incident ray with the normal to the mirror aperture plane. Using simple geometrical optics the following equation can be derived for the ray reflected at the point B:

$$y = my + c \tag{5}$$

where:

$$m = \tan(90 + 2I - \theta), \quad \text{for } X_n \geqslant 0, \tag{6a}$$

$$m = \tan(90 - 2I - \theta), \quad \text{for } X_n < 0, \quad \text{and} \tag{6b}$$

$$c = Y_n - m(X_n). \tag{7}$$

The coordinates of the intersection point $L(X_p, Y_p)$ of the reflected ray (Eq. (5)) for two absorber configurations can be given by the following equations:

– flat-horizontal absorber

$$X_p = (f - Y_n + mX_n)/m, \tag{8}$$

$$Y_p = f \tag{9}$$

– flat-vertical absorber

$$X_p = 0, \tag{10}$$

$$Y_p = m(X_p - X_n) + Y_n. \tag{11}$$

If the ray is not captured within the prespecified dimensions of the absorber, it is either reflected for the second time from the mirror surface or is lost due to the smaller size of the absorber. In such a situation, in order to trace the path of this ray after first reflection, the coordinates of the intersection points of this ray with the mirror are determined from Eq. (5).

On the coordinates of the point a which there occurs the second reflection are known, the equation of the reflected ray at this point can be obtained by the following procedure similar to that used in the case of the first reflection. The procedure outlined above is then used to obtain the final point of the ray interception on the surface of the absorber for both of its configurations.

In order to study the distribution of the local concentration ratio (LCR) on the absorber surface, the absorber cross-section is divided into a large number of zones of equal width. The LCR is calculated as the ratio of the sum of the effective contribution of all the rays intercepted by a typical zone of the absorber to the total number of rays incident on a zone of equal width in the entrance aperture. Within the framework of the ray optical model presented in this work, the effective

contribution CI_{eff} of each ray would depend on the number of its reflections (z) from the mirror surface prior to interception by the absorber, and on the reflectance (ϱ) of the mirror. Thus

$$CI_{eff} = \varrho^z. \tag{12}$$

A smooth LCR curve may be finally obtained by assigning the LCR of all the zones their respective midpoints.

3. Results and discussion

3.1. Flat-horizontal absorber

Figure 2 shows the distribution of the local concentration ratio on the plane of the flat-horizontal absorber for a normal incidence of solar radiation ad for four different values of mirror rim angle. The distance represented by the x-axis is measured from the centre of the absorber, placed in the paraxial focal plane. For all the values of the mirror rim angle, the aperture diameter is kept constant (1.00 m). Thus, the amount of solar energy incident on the aperture of the concentrator is the same in all the cases. This distribution is studied for all the rays captured on the lower surface of the absorber plane (facing the vertex of the mirror). For the case of normally incident rays the maximum value of the angle of incidence I is determined by the mirror rim angle, and the larger the angle of incidence, the greater the distance of the interception point $L(X_p, Y_p)$ of the reflected ray from the centre of the absorber. Therefore, at lower values of mirror rim angle, all the rays are captured nearer the absorber centre leading to a high concentration of energy in that region. A mirror with a larger rim angle has also a lower relative aperture, therefore the absorber is placed closer to the mirror surface. Thus, a certain fraction of the reflected rays which strike the upper surface of the absorber plane do not contribute to the LCR plotted in Fig. 2. For larger mirror rim angles a greater number of rays undergo

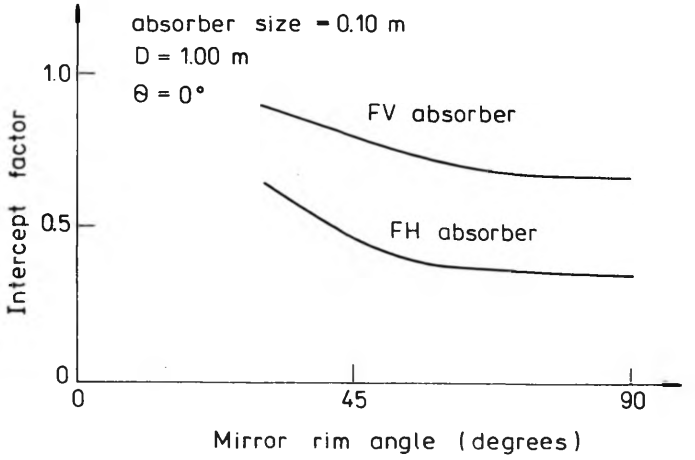

Fig. 2. LCR distribution on the plane of the flat-horizontal absorber for different values of mirror rim angle

multiple reflections, hence the contribution of these rays to the LCR is reduced. These factors are responsible for the decrease in the peak LCR with the increasing mirror rim angle. Secondary peak observed in the curves LCR for mirror rim angles are equal to 60 and 90 degrees, due to the rays undergoing multiple reflections at the mirror surface before being intercepted by the absorber plane.

Figure 3 shows the effect of the mirror rim angle on the intercept factor for the absorber of size 0.10 m, with the shading of the mirror due to finite size of the absorber being taken into account.

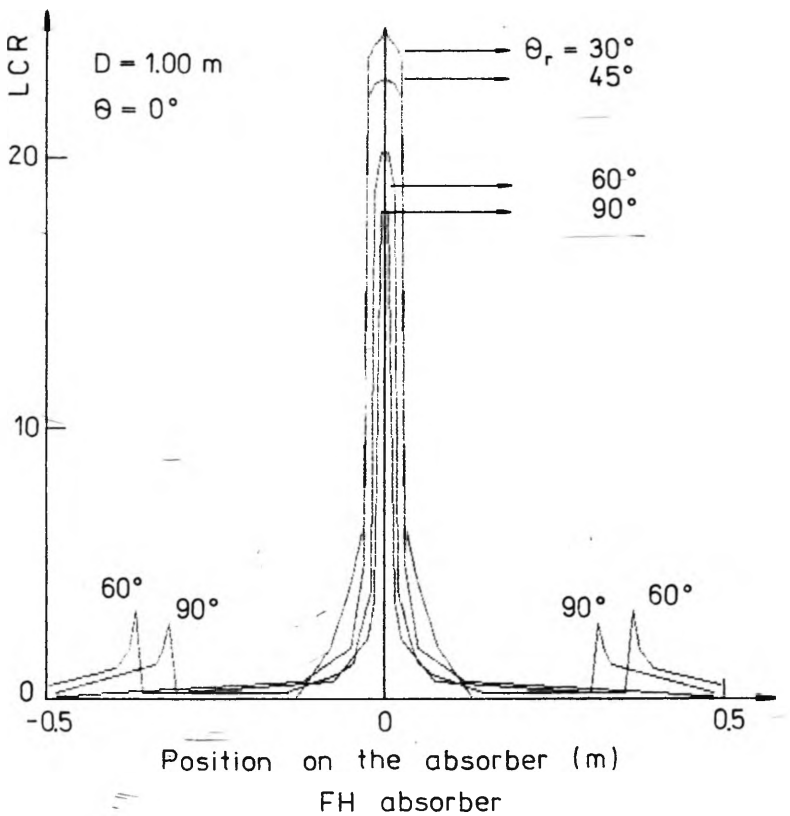

Fig. 3. Variation of the intercept factor with the mirror rim angle for both flat-horizontal and flat-vertical absorbers

Figure 4 shows the effect of defocusing the absorber plane by Δy on the distribution of the local concentration ratio on the defocused absorber plane.

Figure 5 shows the effect of variation of the solar radiation incidence angle θ with the normal to the aperture plane, on the LCR distribution on the absorber plane. With the increasing value of θ, the peak value of the LCR distribution decreases being accompanied with a shift in the position of the peak. The direction of the peak depends on the position of the sun during the day.

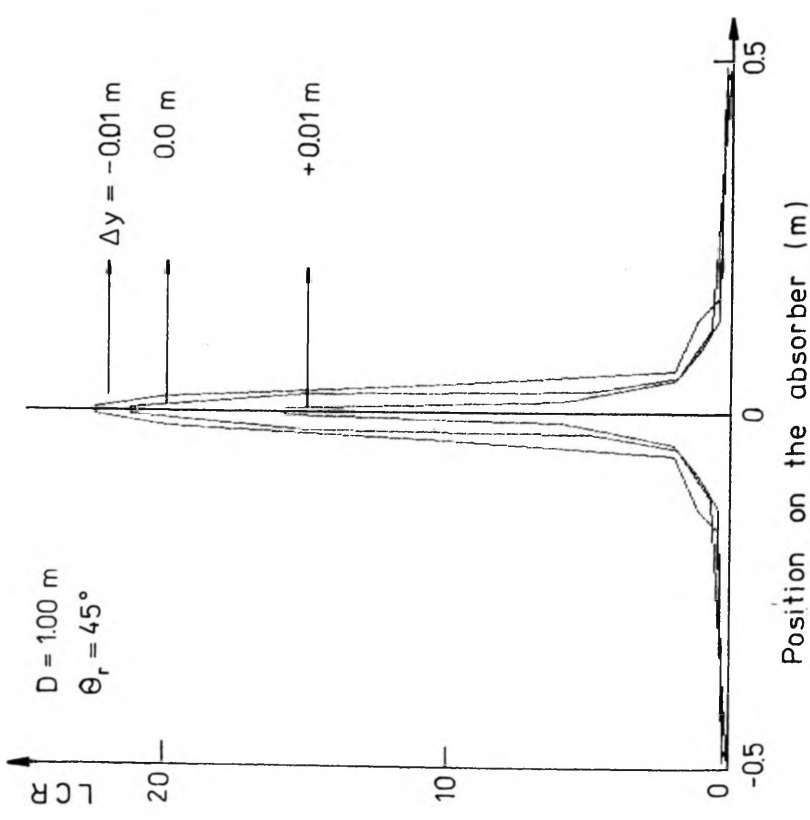

Fig. 4. LCR distribution on the defocused plane of a flat-horizontal absorber

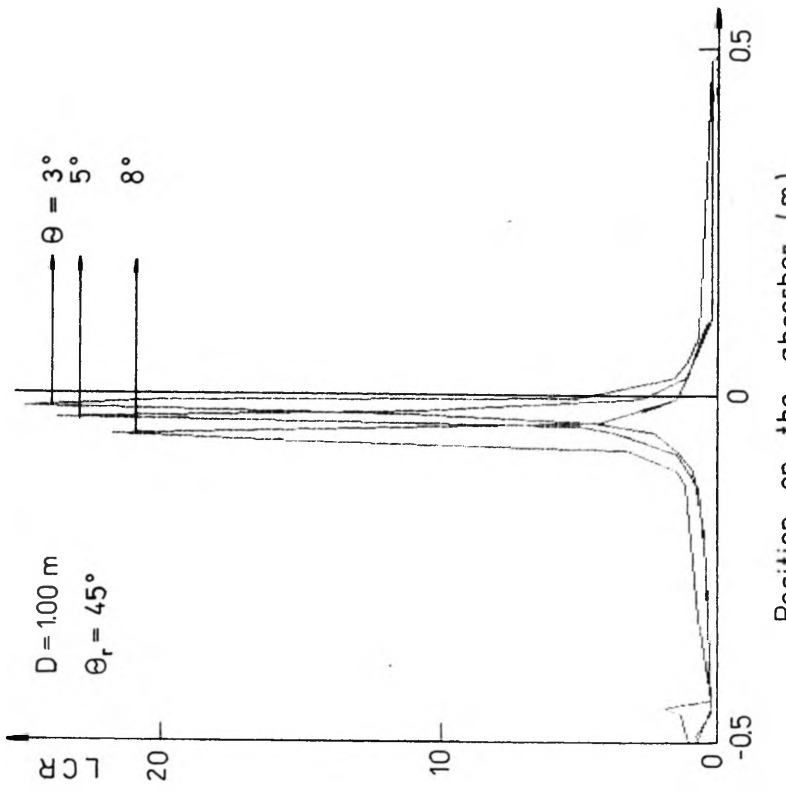

Fig. 5. LCR distribution on the plane of the flat-horizontal absorber for different values of the solar radiation incidence angles

3.2. Flat-vertical absorber

Figure 6 shows the LCR distribution on the plane of the flat-vertical absorber for four different mirror rim angles and normal incidence of the solar radiation. The left and right halves of the figure represent the distribution on the respective surfaces of the absorber. For all the values of the mirror rim angle, the aperture diameter is kept constant (1.00 m). The distance presented on the x-axis is measured from the vertex of the mirror along the optical axis. In this case, an increase in the mirror rim angle results also in a decrease in the peak LCR. A secondary peak on the LCR curve is observed for the mirror rim angle of 90 degrees. This is again due to the rays which undergo multiple reflections before being intercepted by the absorber.

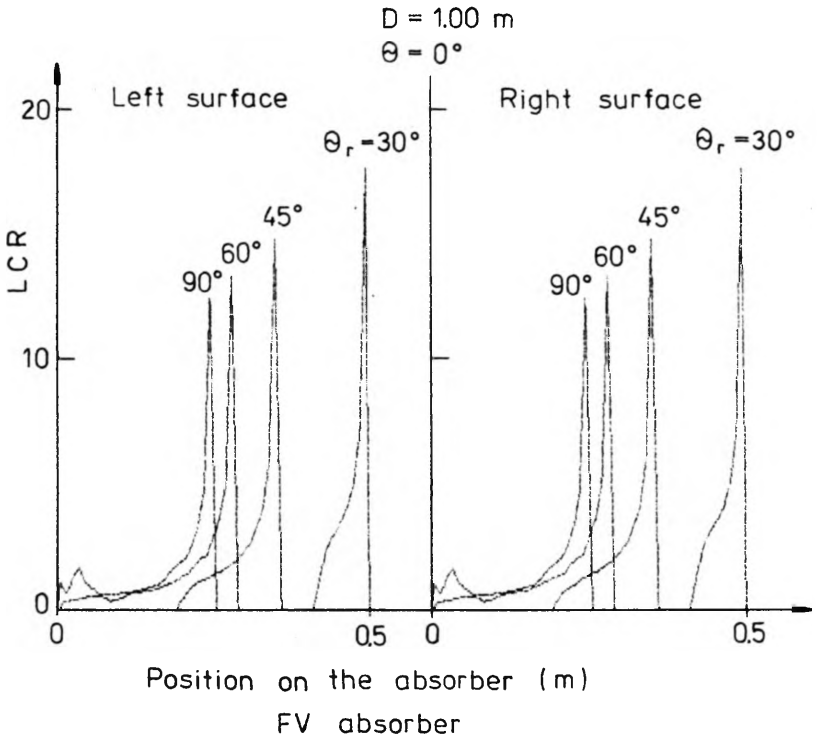

Fig. 6. LCR distribution on the left and right surfaces of the flat-vertical absorber for different values of mirror rim angle

The effect of the mirror rim angle on the intercept factor for a flat-vertical absorber of size 0.10 m is also shown in Fig. 3.

The effect of lateral shift of the absorber plane (for normal incidence of solar radiation) on the LCR distribution on the shifted plane is depicted in Fig. 7. When the absorber plane is shifted from the mirror vertex by Δx in the positive x-direction, then the peak LCR on the right surface of the absorber increases, with the peak being shifted to the left from its initial position. Simultaneously, the peak LCR on the left

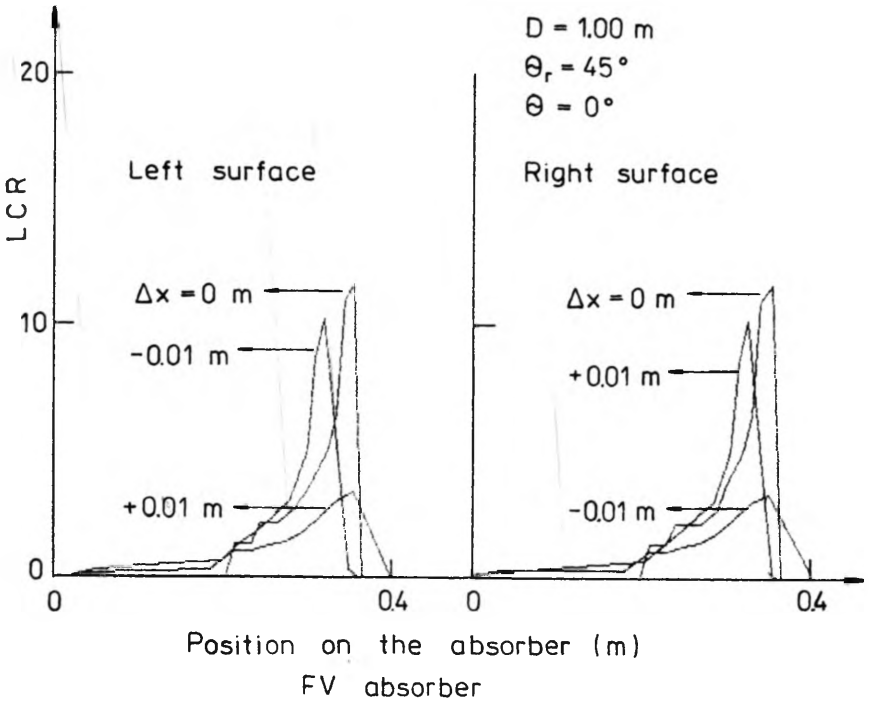

Fig. 7. LCR distribution on the left and right surfaces of a laterally shifted flat-vertical absorber

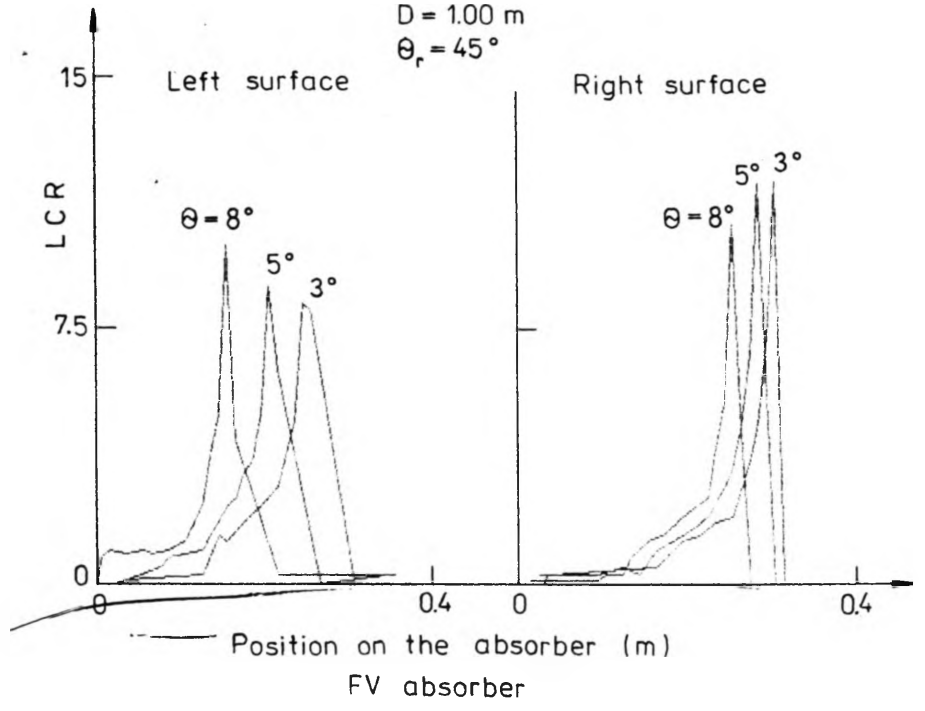

Fig. 8. LCR distribution on the left and right surfaces of the flat-vertical absorber for different values of solar radiation incidence angles

surface of the absorber decreases, with the peak being shifted to the right from its inital position. Similar results are observed when the absorber plane is shifted by the same quantity in the negative x-direction from the mirror vertex, but the LCR distribution on the absorber surfaces is interchanged.

Figure 8 depicts the effect of variation of the solar radiation incidence angle θ with the normal to the aperture plane, on the LCR distribution on the absorber plane. With an increase in the value of θ, the peak value of LCR on the left surface of the absorber increases, being accompanied with a shift in the peak LCR. Simultaneously, on the right surface of the absorber, one observes a decrease in the peak value of the LCR with an increase in the value of θ. The position of this peak shifts in a direction opposite to the shift noted on the left surface of the absorber.

Reference

[1] TABOR H., ZEIMER H., Solar Energy **6** (1962), 55.

Received August 18, 1988
in revised form January 25, 1989

Характеристика концентрации колесно-цилиндрического солнечного концентратора, сезонно регулируемого

Характеристику концентрации колесно-цилиндрического солнечного концентратора исследовали для двух конфигураций абсорбера: плоско-горизонтального и плоско-вертикального. Употребили конвенциональную технику расчета хода лучей. Из-за того, что концентратор действует при сезонной регуляции, кривые распределения вычерчены для разных значений угла падения. Исследовали влияние угла борта зеркала, дефокусировки абсорбера, поперечного перемещения, а также светомаскировки, вызванной абсорбером, на характеристику концентрации.